MATHEMATICAL BIOSCIENCES
AND ENGINEERING
Volume **12**, Number **6**, December **2015**

doi:10.3934/mbe.2015.12.1173

pp. **1173–1187**

MATHEMATICAL MODEL AND ITS FAST NUMERICAL METHOD FOR THE TUMOR GROWTH

Hyun Geun Lee

Institute of Mathematical Sciences, Ewha Womans University
Seoul 120-750, Korea

Yangjin Kim

Department of Mathematics, Konkuk University
Seoul 143-701, Korea

Junseok Kim

Department of Mathematics, Korea University
Seoul 136-713, Korea

Abstract. In this paper, we reformulate the diffuse interface model of the tumor growth (S.M. Wise *et al.*, Three-dimensional multispecies nonlinear tumor growth-I: model and numerical method, J. Theor. Biol. 253 (2008) 524–543). In the new proposed model, we use the conservative second-order Allen–Cahn equation with a space–time dependent Lagrange multiplier instead of using the fourth-order Cahn–Hilliard equation in the original model. To numerically solve the new model, we apply a recently developed hybrid numerical method. We perform various numerical experiments. The computational results demonstrate that the new model is not only fast but also has a good feature such as distributing excess mass from the inside of tumor to its boundary regions.

1. **Introduction.** The morphological evolution of a growing tumor is the result of many factors, such as cell–cell and cell–matrix adhesion, mechanical stress, cell motility, and transport of oxygen, nutrients, and growth factors [3]. Mathematical modeling of cancer gives unique and important insights into tumor progression, helps explain experimental and clinical observations, and helps provide optimal treatment strategies [24]. In the past several years, a considerable amount of research on mathematical models of cancer has been conducted, and numerical simulations of tumor growth have been performed [6, 10, 15, 25, 26, 29, 31, 34, 36, 38, 40, 41, 47, 49, 52, 54, 55, 56, 59, 63]. A variety of modeling strategies are available to investigate one or more aspects of cancer. Discrete cell-based models (e.g., cellular automata [2, 9, 30, 44, 46, 62] and agent-based models [7, 43, 50]), where individual cells are tracked and updated according to a specific set of biophysical rules, are particularly useful for studying carcinogenesis, natural selection, genetic instability, and interactions of individual cells with each other and the microenvironment. In larger-scale systems, continuum methods provide a good modeling alternative [14, 16, 17, 18, 19, 27, 37, 39, 48]. The governing equations are typically of the reaction–diffusion type. Recently, nonlinear continuum modeling has been

2010 *Mathematics Subject Classification.* Primary: 65M06; Secondary: 92B05.

Key words and phrases. Tumor growth, conservative Allen–Cahn equation, operator splitting method, multigrid method.

performed to study the effects of shape instabilities on avascular, vascular, and angiogenic solid tumor growth. Cristini *et al.* [27] performed the first fully nonlinear simulations of a continuum model of avascular and vascularized tumor growth in two dimensions using a boundary integral method. Li *et al.* [48] extended this model to three dimensions using an adaptive boundary integral method. Zheng *et al.* [65] also extended this model to include a hybrid continuum discrete model of angiogenesis (based on earlier work of Anderson and Chaplain [5]) and investigated the nonlinear coupling between growth and angiogenesis in two dimensions using finite element/level-set method. Wise *et al.* simulated tumor growth [64] and angiogenesis [35] in three dimensions using a diffuse interface, multiphase mixture model. Chen *et al.* [24] extended the model of Wise *et al.* and incorporated the effect of a stiff membrane to model tumor growth in a confined microenvironment.

Here, we reformulate the diffuse interface continuum model of multispecies tumor growth of Wise et al. [64]. The model consists of fourth-order nonlinear advection–reaction–diffusion equations of Cahn–Hilliard-type (CH) [21] for the cell species volume fractions coupled with reaction–diffusion equations for the substrate components. Because the original model involves fourth-order equations, it is challenging to develop accurate and efficient numerical methods. For example, explicit methods suffer from severe time step restrictions ($\Delta t < C(\Delta x)^4$) and thus are computationally expensive to handle large systems. Therefore, in the new proposed model, we use the conservative second-order Allen–Cahn (AC) equation with a space–time dependent Lagrange multiplier instead of using the fourth-order CH equation in the original model. The classical AC equation was originally introduced as a phenomenological model for antiphase domain coarsening in a binary alloy [4], but does not conserve mass of the mixture. Rubinstein and Sternberg [57] introduced a nonlocal AC equation with a time dependent Lagrange multiplier to enforce conservation of mass. However, with their model, it is difficult to keep small features since they dissolve into the bulk region. One of the reasons for this is that mass conservation is realized by a global correction using the time-dependent Lagrange multiplier. To resolve the problem, we use a space–time dependent Lagrange multiplier to preserve the mass of the mixture. And, to numerically solve the new model, we use a recently developed hybrid numerical method [45].

This paper is organized as follows. In Section 2, we reformulate the diffuse interface model of Wise *et al.* [64] by using the conservative second-order AC equation with a space–time dependent Lagrange multiplier. A numerical algorithm using an operator splitting method is described in Section 3. Various numerical experiments are presented in Section 4. Finally, conclusions are drawn in Section 5.

2. Mathematical model.

In this section, we present a mathematical model of tumor growth. We begin by recalling the nondimensional tumor growth model from Wise *et al.* [64], where a thermodynamically consistent diffuse interface continuum model of multispecies tumor growth was developed, analyzed, and simulated. The authors take into account mechanical interactions, mainly focused on cell–cell adhesion between a tumor and host. The dimensionless dependent variables defined in a bounded tissue domain $\Omega \subset \mathbb{R}^d$ ($d = 2$ or 3) are as follows: ϕ, ψ, and ξ are the volume fractions of tumor cells, dead tumor cells, and host tissue, respectively (see Figure 1). Here, we note that $\phi - \psi$ is the volume fraction of viable tumor cells. Hence, ϕ is the sum of the volume fractions of viable and dead tumor cells. $\mathbf{u}$, p, and n are the tumor velocity, pressure, and nutrient concentration, respectively.

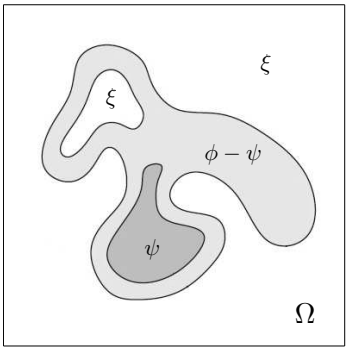

FIGURE 1. Schematic of a growing tumor. ϕ and ψ are the volume fractions of the tumor and dead tumor cells, respectively. ξ is the volume fraction of the host tissue.

The original governing equations for the tumor growth in [64] are

$$\frac{\partial \phi}{\partial t} = M\nabla\cdot(\phi\nabla\mu) - \nabla\cdot(\phi\mathbf{u}) + \phi S_T, \tag{1}$$

$$\mu = F'(\phi) - \epsilon^2\Delta\phi, \tag{2}$$

$$\frac{\partial \psi}{\partial t} = M\nabla\cdot(\psi\nabla\mu) - \nabla\cdot(\psi\mathbf{u}) + \phi S_D, \tag{3}$$

$$\mathbf{u} = -\nabla p - \frac{\gamma}{\epsilon}\phi\nabla\mu, \tag{4}$$

$$\nabla\cdot\mathbf{u} = S_T, \tag{5}$$

$$0 = \nabla\cdot(D(\phi)\nabla n) + T_C(\phi, n) - \nu_U n(\phi - \psi), \tag{6}$$

where $M > 0$ is a mobility, μ is the chemical potential, $F(\phi) = \phi^2(1-\phi)^2/4$ is a double well bulk energy, $\epsilon > 0$ is a parameter related to the thickness of the diffuse interface that separates the tumor and host domains, and γ is a parameter related to the cell–cell adhesion force. S_T and S_D are the net sources of tumor and dead cells, respectively, and are defined as

$$S_T = \lambda_M n(\phi - \psi) - \lambda_L\psi \quad \text{and} \quad S_D = (\lambda_A + \lambda_N\mathcal{H}(n_N - n))(\phi - \psi) - \lambda_L\psi,$$

where λ_M, λ_L, λ_A, and λ_N are the rates of volume gain or loss due to cellular mitosis, lysing, apoptosis, and necrosis, respectively, $\mathcal{H}$ is a Heaviside step function, and n_N is the nutrient limit for cell viability. The diffusion coefficient $D(\phi)$ and nutrient capillary source term $T_C(\phi, n)$ are, respectively,

$$D(\phi) = D_H(1 - Q(\phi)) + Q(\phi)$$
$$\text{and} \quad T_C(\phi, n) = \left(\nu_p^H(1 - Q(\phi)) + \nu_p^T Q(\phi)\right)(n_c - n),$$

where D_H is the nondimensional nutrient diffusion coefficient in the host domain, ν_p^H and ν_p^T denote the nutrient transfer rates for preexisting vascularization in the host and tumor domains, respectively, and n_c is the nutrient level in the capillaries. $Q(\phi)$ is an interpolation function and is defined as

$$Q(\phi) = \begin{cases} 1 & \text{if } 1 \le \phi \\ 3\phi^2 - 2\phi^3 & \text{if } 0 < \phi < 1 \\ 0 & \text{if } \phi \le 0, \end{cases}$$

with $Q(1) = 1$, $Q(1/2) = 1/2$, and $Q(0) = 0$. ν_U is the nutrient uptake rate by the viable tumor cells. Eqs. (1)–(6) are valid on the whole domain Ω and not just on the tumor volume. There are no boundary conditions required for ϕ and ψ at the tumor boundary. At the outer boundary, we choose the following boundary conditions

$$\mathbf{n} \cdot \nabla\phi = \mathbf{n} \cdot \nabla\psi = \mu = \mathbf{n} \cdot \nabla p = 0, \ n = 1 \text{ on } \partial\Omega,$$

where $\mathbf{n}$ is the unit normal vector to $\partial\Omega$.

The diffuse interface model of Wise *et al.* [64] involves the fourth-order CH Eq. (1) and (2) with a source term. In this paper, we propose an alternative model for Eqs. (1) and (2). The proposed model consists of the following two equations and Eqs. (3)–(6):

$$\frac{\partial\phi}{\partial t} = -\nabla \cdot (\phi\mathbf{u}) + \phi S_T, \tag{7}$$

$$\frac{\partial\phi}{\partial t} = M\phi\left(-F'(\phi) + \epsilon^2\Delta\phi + \beta(t)F(\phi)\right). \tag{8}$$

First, we update ϕ according to Eq. (7), and then we relax ϕ using Eq. (8). In Eq. (8),

$$\frac{\partial\phi}{\partial t} = -F'(\phi) + \epsilon^2\Delta\phi$$

is the classical AC equation which was originally introduced as a phenomenological model for antiphase domain coarsening in a binary alloy [4]. Since the classical AC equation does not have the mass conservation property, Brassel and Bretin [11] introduced a nonlocal AC equation with a space–time dependent Lagrange multiplier $(\beta(t)\sqrt{F(\phi)})$ to enforce conservation of mass. Here, $\beta(t)$ satisfies $\beta(t) = \int_\Omega F'(\phi)\, d\mathbf{x} / \int_\Omega F(\phi)\, d\mathbf{x}$. The proposed model involves a second-order equation and we will apply the recently developed hybrid numerical method [45] to numerically solve it.

3. Numerical solution.

In this section, we describe an operator splitting algorithm for solving Eqs. (3)–(8). For simplicity and clarity of exposition, we shall discretize Eqs. (3)–(8) in two-dimensional space, i.e., $\Omega = (a, b) \times (c, d)$. Three-dimensional discretization is defined analogously. Let the computational domain be partitioned into a uniform mesh with mesh spacing h. The center of each cell, Ω_{ij}, is located at $(x_i, y_j) = ((i - 0.5)h, (j - 0.5)h)$ for $i = 1, \ldots, N_x$ and $j = 1, \ldots, N_y$. N_x and N_y denote the number of cells in the x- and y-directions, respectively. Cell vertices are located at $(x_{i+\frac{1}{2}}, y_{j+\frac{1}{2}}) = (ih, jh)$. In this paper, tumor and dead cells, pressures, and nutrients are stored at the cell centers and velocities at cell faces. Let ϕ_{ij}^k be the approximations of $\phi(x_i, y_j, k\Delta t)$, where $\Delta t = T/N_t$ is the time step, T is the final time, and N_t is the total number of time steps. The other terms are similarly defined.

In this paper, we use an operator splitting method, in which we numerically solve Eqs. (7) and (8) by solving successively a sequence of simpler problems:

$$\frac{\partial\phi}{\partial t} = -\nabla \cdot (\phi\mathbf{u}) + \phi S_T, \tag{9}$$

$$\frac{\partial\phi}{\partial t} = M\phi\epsilon^2\Delta\phi, \tag{10}$$

$$\frac{\partial\phi}{\partial t} = -M\phi F'(\phi), \tag{11}$$

$$\frac{\partial \phi}{\partial t} = M\phi\beta(t)F(\phi). \tag{12}$$

First, we solve Eq. (9) by applying the explicit Euler's method:

$$\frac{\phi_{ij}^{k+1,1} - \phi_{ij}^{k}}{\Delta t} = -\nabla_d \cdot (\phi^k \mathbf{u}^k)_{ij} + \phi_{ij}^k S_T{}_{ij}^k,$$

where $\nabla_d \cdot$ is the discrete divergence operator. Next, we solve Eq. (10) by applying the explicit Euler's method:

$$\frac{\phi_{ij}^{k+1,2} - \phi_{ij}^{k+1,1}}{\Delta t} = M^k \epsilon^2 \Delta_d \phi_{ij}^{k+1,1},$$

where $M^k = M\phi_{ij}^k$ and Δ_d is the discrete Laplacian operator. And Eq. (11) is solved analytically using the method of separation of variables [60] and the solution is given as

$$\phi_{ij}^{k+1,3} = 0.5 + \frac{\phi_{ij}^{k+1,2} - 0.5}{\sqrt{e^{-0.5M^k\Delta t} + (2\phi_{ij}^{k+1,2} - 1)^2\left(1 - e^{-0.5M^k\Delta t}\right)}}.$$

Finally, we discretize Eq. (12) as

$$\frac{\phi_{ij}^{k+1} - \phi_{ij}^{k+1,3}}{\Delta t} = M^k \beta^{k+1,3} F(\phi_{ij}^{k+1,3}). \tag{13}$$

By Eq. (13), we get $\phi_{ij}^{k+1} = \phi_{ij}^{k+1,3} + \Delta t M^k \beta^{k+1,3} F(\phi_{ij}^{k+1,3})$, then by the property of mass conservation

$$\sum_{i=1}^{N_x}\sum_{j=1}^{N_y} \phi_{ij}^{k+1,1} = \sum_{i=1}^{N_x}\sum_{j=1}^{N_y} \phi_{ij}^{k+1} = \sum_{i=1}^{N_x}\sum_{j=1}^{N_y} \left(\phi_{ij}^{k+1,3} + \Delta t M^k \beta^{k+1,3} F(\phi_{ij}^{k+1,3})\right).$$

Thus,

$$\beta^{k+1,3} = \frac{1}{\Delta t}\sum_{i=1}^{N_x}\sum_{j=1}^{N_y}\left(\phi_{ij}^{k+1,1} - \phi_{ij}^{k+1,3}\right) \Big/ \sum_{i=1}^{N_x}\sum_{j=1}^{N_y} M^k F(\phi_{ij}^{k+1,3}).$$

Eqs. (3)–(6) are discretized as

$$\begin{aligned}
\frac{\psi_{ij}^{k+1} - \psi_{ij}^{k}}{\Delta t} &= \nabla_d \cdot (M\psi^k \nabla_d \mu^{k+1})_{ij} - \nabla_d \cdot (\psi^k \mathbf{u}^k)_{ij} + \phi_{ij}^k S_D{}_{ij}^k, \\
u_{i+\frac{1}{2},j}^{k+1} &= -D_x p_{i+\frac{1}{2},j}^{k+1} - \frac{\gamma}{\epsilon}(\phi^{k+1} D_x \mu^{k+1})_{i+\frac{1}{2},j}, \qquad (14)\\
v_{i,j+\frac{1}{2}}^{k+1} &= -D_y p_{i,j+\frac{1}{2}}^{k+1} - \frac{\gamma}{\epsilon}(\phi^{k+1} D_y \mu^{k+1})_{i,j+\frac{1}{2}}, \qquad (15)\\
\nabla_d \cdot \mathbf{u}_{ij}^{k+1} &= S_T{}_{ij}^{k+1}, \\
0 &= \nabla_d \cdot (D(\phi^{k+1})\nabla_d n^{k+1})_{ij} + T_C(\phi_{ij}^{k+1}, n_{ij}^{k+1}) \\
&\quad -\nu_U n_{ij}^{k+1}(\phi_{ij}^{k+1} - \psi_{ij}^{k+1}), \qquad (16)
\end{aligned}$$

where u and v are the horizontal and vertical components of $\mathbf{u}$, respectively. The discrete differentiation operators are

$$D_x p_{i+\frac{1}{2},j} = \frac{p_{i+1,j} - p_{ij}}{h} \quad \text{and} \quad D_y p_{i,j+\frac{1}{2}} = \frac{p_{i,j+1} - p_{ij}}{h},$$

and ∇_d is the discrete gradient operator. Apply the divergence operator to Eqs. (14) and (15) and get a Poisson equation for p_{ij}^{k+1}:

$$\Delta_d p_{ij}^{k+1} = -\frac{\gamma}{\epsilon}\nabla_d \cdot (\phi^{k+1}\nabla_d \mu^{k+1})_{ij} - {S_T}_{ij}^{k+1}. \tag{17}$$

The resulting linear systems of Eqs. (16) and (17) are solved by a fast solver, such as a linear multigrid method [12, 61].

4. Numerical experiments.

4.1. Time scaling between the Cahn–Hilliard and conservative Allen–Cahn models.

In this paper, we use the conservative second-order Allen–Cahn (CAC) equation with a space–time dependent Lagrange multiplier instead of using the fourth-order Cahn–Hilliard (CH) equation in the original model. The CAC, constant mobility CH, and variable mobility CH equations provide an approximation to motion by the volume preserving mean curvature flow [8, 11, 13, 42, 58], the Mullins–Sekerka flow [1, 22, 23, 28, 33, 53], and the surface diffusion flow [20, 32, 51], respectively. Thus, there is a need for a time scaling to consider a difference between the motion of the interface for the CAC, constant mobility CH, and variable mobility CH equations. To evaluate a time scaling between the CH (Eqs. (1) and (2)) and CAC (Eqs. (7) and (8)) models, we consider the following initial condition:

$$\phi(x, y, 0) = \frac{1}{2}\left[1 + \tanh\left(\frac{4 - \sqrt{(x-10)^2/1.4 + (y-10)^2}}{2\sqrt{2}\epsilon}\right)\right]$$

on a domain $\Omega = [0, 20] \times [0, 20]$, with $h = 20/128$, $\Delta t = 0.01$, and $\epsilon = 0.1\sqrt{2}$. In this test, the effects of velocity $\mathbf{u}$ and net source of tumor cells S_T are negligible and we consider a constant mobility case. The numerical solution is computed to time $T = 200$.

Figures 2 (a) and (b) show the time evolutions of $y = 10$ of 0.5-level of ϕ obtained by solving the CH and CAC equations without and with time scaling, respectively. Here, a time scaling factor is about 3.2, that is, $M_{\mathrm{CAC}} = 3.2 M_{\mathrm{CH}}$, where M_{CH} and M_{CAC} are constant mobilities of the CH and CAC equations, respectively. Note that the time scaling factor depends on the initial morphology of the interface.

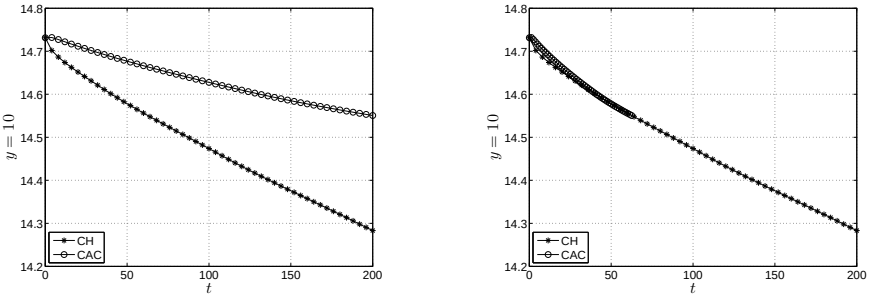

(a) Without time scaling (b) With time scaling

FIGURE 2. Time evolutions of $y = 10$ of 0.5-level of ϕ obtained by solving the CH and CAC equations.

4.2. **Comparison between the Cahn–Hilliard and conservative Allen–Cahn models.** To compare the dynamics between the CH and CAC models, we take the following initial condition:

$$\phi(x,y,0)=\frac{1}{2}\left[1+\tanh\left(\frac{2-\sqrt{(x-10)^2/1.4+(y-10)^2}}{2\sqrt{2}\epsilon}\right)\right] \tag{18}$$

on a domain $\Omega=[0,20]\times[0,20]$. Here, we use $h=20/128$, $\Delta t=0.01$, and $\epsilon=0.1\sqrt{2}$. In this simulation, we solve Eqs. (1)–(6) (the CH model) and (3)–(8) (the CAC model) with the following parameters: $M=10$ for the CH model, $M=32$ for the CAC model, $\gamma=0.0$, $\nu_U=1.0$, $\lambda_M=8.0$, $\lambda_L=1.0$, $\lambda_A=0.0$, $\lambda_N=3.0$, $n_N=0.6$, $D_H=1.0\times10^3$, $\nu_p^H=0.0$, $\nu_p^T=0.0$, and $n_c=1.0$. Note that we take the same parameter values as in [64] except for λ_M. To investigate the difference in distributing excess mass, we choose 8 times larger than the value in [64].

Figures 3 and 4 show the time evolutions of tumor cells obtained by solving the CH and CAC models, respectively. As we can see in Figure 3, the CH model does not distribute well excess mass from the inside of tumor to its boundary regions and thus excess mass builds up inside and the volume fraction of tumor cells becomes much larger than one. On the other hand, in the CAC model, excess mass (obtained by solving Eq. (9)) diffuses according to Eq. (10) and then the volume fraction of tumor cells becomes close to one according to Eq. (11). Finally, mass (changed by the AC step (10) and (11)) is corrected in the interfacial region by the mass correction step (12). Therefore, excess mass is well distributed to boundary regions of tumor cells.

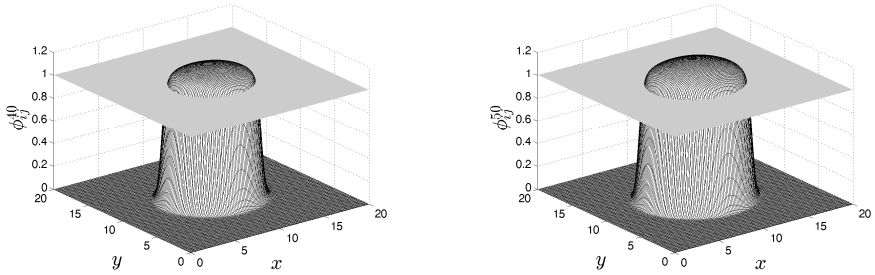

(a) ϕ_{ij}^{40} (b) ϕ_{ij}^{50}

FIGURE 3. Time evolutions of tumor cells obtained by solving the CH model.

4.3. **Two-dimensional tumor growth.** In this section, we present two-dimensional simulations of tumor growth using the parameters given in Table 1. Because the diffusivity of the nutrient in the host medium is 1000 times larger than that in the tumor interstitium, we use $D(\phi)$ as in [64]

$$D(\phi)=1+(D_H-1)(1-\phi)^8.$$

To validate our new model and numerical algorithm, we take the same initial condition (18) as in the previous section on a domain $\Omega=[0,20]\times[0,20]$. $h=20/256$, $\Delta t=0.01$, and $\epsilon=0.1$ are used.

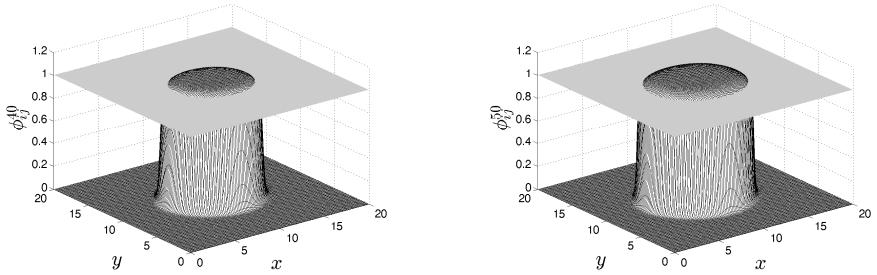

(a) ϕ_{ij}^{40} (b) ϕ_{ij}^{50}

FIGURE 4. Time evolutions of tumor cells obtained by solving the CAC model.

TABLE 1. Nondimensional parameters used in the two-dimensional numerical simulations.

M	10	γ	0.0	ν_U	1.0	λ_M	1.0
λ_L	1.0	λ_A	0.0	λ_N	3.0	n_N	0.6
D_H	1.0×10^3	ν_p^H	0.0	ν_p^T	0.0	n_c	1.0

Figure 5 shows the evolution of the tumor. Initially, there are no dead cells in the tumor. But, as the nutrient concentration falls below level needed for viability, dead cells quickly begin to accrue. At time $t = 5$, the tumor has a fully developed necrotic core. One can observe a slight bulge oriented along the x-direction. At later times, the instability becomes more pronounced and the tumor develops buds that elongate into protruding fingers. The instability enables the tumor to increase its exposure to nutrient as its surface area increases relative to its volume. This allows the tumor to overcome the diffusional limitations to growth. The tumor will grow indefinitely as the instability repeats itself on the buds and protruding fingers. This result is in good agreement with the result in [64]. Furthermore, during the simulation, our new model (3)–(8) and numerical method take $500.624s$ CPU time, whereas the CH-type model (1)–(6) and numerical method in [24] take $3034.718s$ CPU time. Since our new model involves a second-order equation and we use the recently developed hybrid numerical method for solving the model, we save significant computational time. In the following subsections, we will investigate the effect of biophysical parameters given in Table 1.

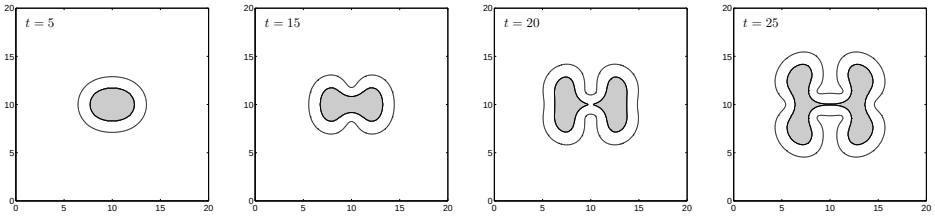

FIGURE 5. Evolution of the contours $\phi - \psi = 0.5$ during growth. The viable tumor cells are primarily contained between the inner and outer contours. The biophysical parameters are given in Table 1.

4.3.1. *Effect of* λ_L. In the net sources S_T and S_D of tumor and dead cells, λ_L is the rate of volume loss due to cellular lysing. Thus, more tumor and dead cells are lysed as λ_L increases, and the more lysed tumor and dead cells translate to the host tissue. To investigate the effect of λ_L, we take the same initial condition (18) and parameter values used to create Figure 5 except for λ_L. We vary λ_L as $\lambda_L = 0.4, 3.0$ and $\lambda_L = 1.0$ (see Figure 5). Figure 6 shows the time evolutions of the tumor for different λ_L values. From the results, we observe that the growth of tumor is inhibited as λ_L increases.

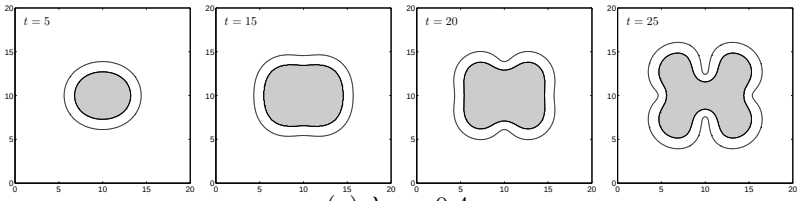

(a) $\lambda_L = 0.4$

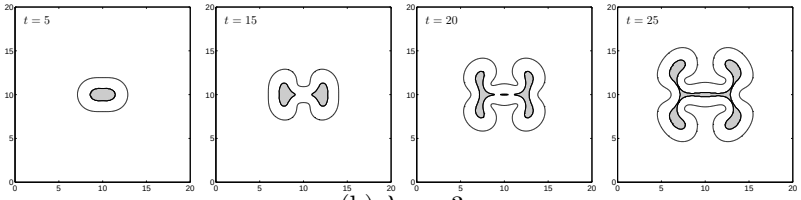

(b) $\lambda_L = 3$

FIGURE 6. Effect of λ_L: Time evolutions of the contours $\phi - \psi = 0.5$ during growth.

4.3.2. *Effect of* n_N. The net source S_D of dead cells is defined as

$$S_D = (\lambda_A + \lambda_N \mathcal{H}(n_N - n))(\phi - \psi) - \lambda_L \psi,$$

where n_N is the nutrient limit for cell viability. When n falls below n_N, tumor cells are dead proportional to λ_N. Thus, more tumor cells translate to dead cells as n_N decreases. To investigate the effect of n_N, we take the same initial condition (18) and parameter values used to create Figure 5 except for n_N. We vary n_N as $n_N = 0.4, 0.8, 0.9$ and $n_N = 0.6$ (see Figure 5). Figure 7 shows the time evolutions of the tumor for different n_N values. As we expected, we can see more and more dead cells as n_N decreases.

4.3.3. *Effect of* ν_p^H *and* ν_p^T. The nutrient capillary source term $T_C(\phi, n)$ is defined as

$$T_C(\phi, n) = \left(\nu_p^H (1 - Q(\phi)) + \nu_p^T Q(\phi)\right)(n_c - n),$$

where ν_p^H and ν_p^T denote the nutrient transfer rates for preexisting vascularization in the host and tumor domains, respectively. As ν_p^H and ν_p^T increase, more nutrients are supplied in the host and tumor domains. In this test, we take the same initial condition (18) and parameter values used to create Figure 5 except for ν_p^H and ν_p^T. Figure 8 shows the evolution of the tumor with $\nu_p^H = \nu_p^T = 0.4$. Since more nutrients are supplied in the host and tumor domains, the tumor grows bigger.

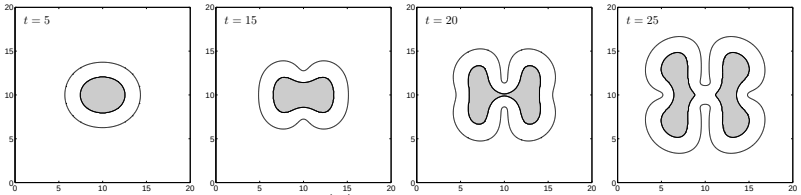

(a) $n_N = 0.4$

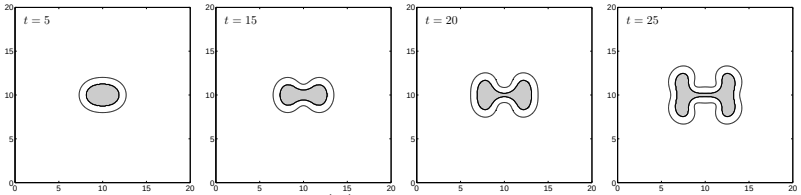

(b) $n_N = 0.8$

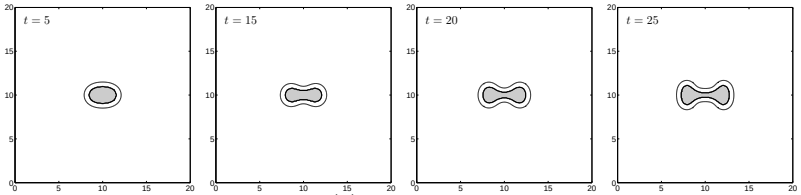

(c) $n_N = 0.9$

FIGURE 7. Effect of n_N: time evolutions of the contours $\phi - \psi = 0.5$ during growth.

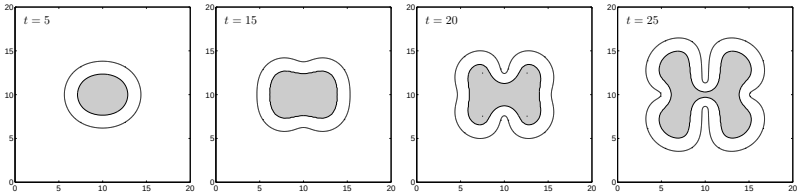

FIGURE 8. Effect of ν_p^H and ν_p^T: evolution of the contours $\phi - \psi = 0.5$ during growth with $\nu_p^H = \nu_p^T = 0.4$.

4.3.4. *Effect of initial condition.* To examine the effect of initial condition, we take the following initial conditions

$$\phi(x, y, 0) = \frac{1}{2}\left[1 + \tanh\left(\frac{2 + 0.1\cos(r\theta) - \sqrt{(x-10)^2 + (y-10)^2}}{2\sqrt{2}\epsilon}\right)\right]$$

with $r = 3, 4$. Here,

$$\theta = \begin{cases} \tan^{-1}\left(\frac{y-10}{x-10}\right) & \text{if } x > 10 \\ \pi + \tan^{-1}\left(\frac{y-10}{x-10}\right) & \text{otherwise.} \end{cases}$$

We choose the parameter values used to create Figure 5. Figure 9 shows the time evolutions of the tumor for different r values. Depending on the initial condition, we can see various patterns of tumor growth.

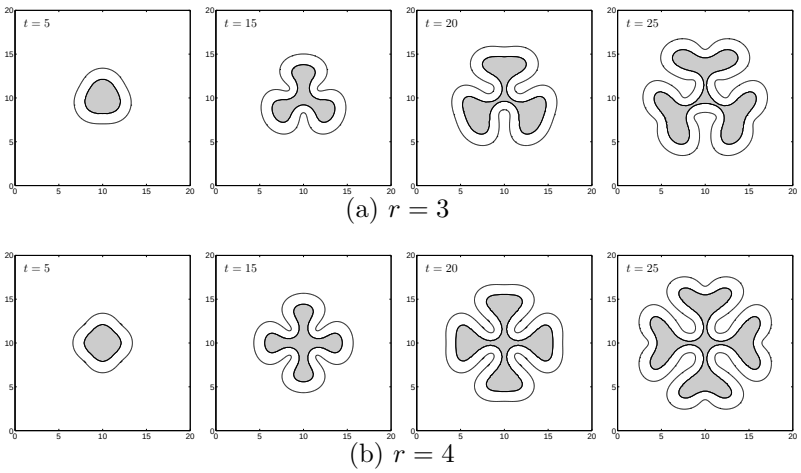

FIGURE 9. Effect of initial condition $\phi(x, y, 0) = 0.5[1 + \tanh((2 + 0.1\cos(r\theta) - \sqrt{(x-10)^2 + (y-10)^2})/(2\sqrt{2}\epsilon))]$: time evolutions of the contours $\phi - \psi = 0.5$ during growth.

4.4. **Three-dimensional tumor growth.** In this paper, we also perform a three-dimensional simulation of tumor growth using the parameters given in Table 1. The initial condition is

$$\phi(x, y, z, 0) = \frac{1}{2}\left[1 + \tanh\left(\frac{2 - \sqrt{(x-10)^2/1.4 + (y-10)^2 + (z-10)^2}}{2\sqrt{2}\epsilon}\right)\right]$$

on a domain $\Omega = [0, 20] \times [0, 20] \times [0, 20]$. $h = 20/128$, $\Delta t = 0.02$, and $\epsilon = 0.1\sqrt{2}$ are used. Figure 10 shows the evolution of the tumor. This simulation demonstrates the capability of feasibly simulating complex tumor progression in three dimensions.

5. **Conclusions.** In this paper, we reformulated the diffuse interface model of the tumor growth of Wise *et al.* [64]. In the new proposed model, we used the conservative second-order Allen–Cahn equation with a space–time dependent Lagrange multiplier instead of using the fourth-order Cahn–Hilliard equation in the original model. To numerically solve the model, we applied a recently developed hybrid numerical method. Through numerical examples, we observed that the new model is not only fast but also has a good feature such as distributing excess mass from the inside of tumor to its boundary regions. We also performed various numerical experiments varying the biophysical parameters.

Acknowledgments. The authors thank the reviewers for the constructive and helpful comments on the revision of this article. The first author (H.G. Lee) was supported by Basic Science Research Program through the National Research Foundation of Korea (NRF) funded by the Ministry of Education (2009-0093827). Y. Kim is supported by the Basic Science Research Program through the National Research Foundation of Korea by the Ministry of Education and Technology (2012R1A1A1043340). The corresponding author (J.S. Kim) was supported by the National Research Foundation of Korea (NRF) grant funded by the Korea government(MSIP) (NRF-2014R1A2A2A01003683).

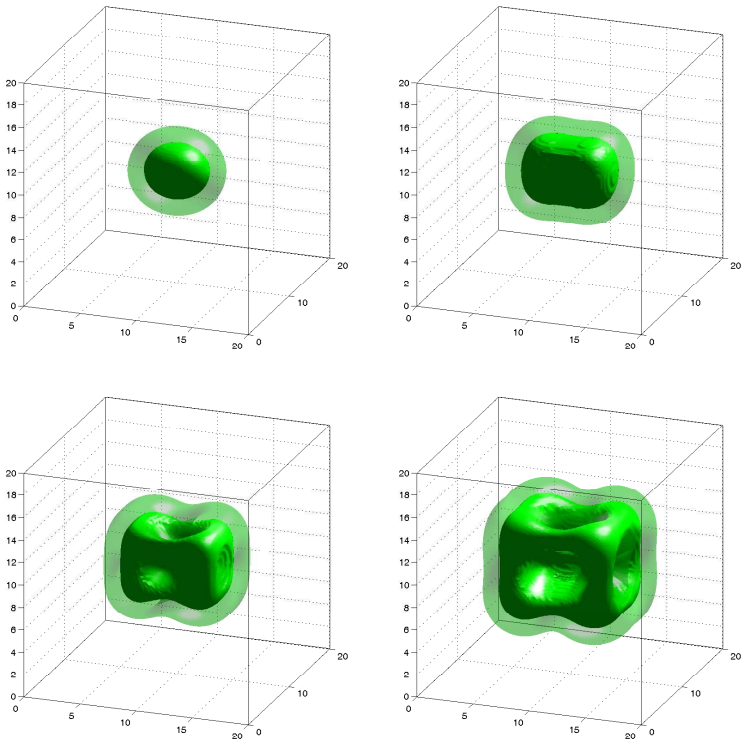

FIGURE 10. Evolution of the contours $\phi - \psi = 0.5$ during growth. The viable cells are primarily contained between the inner and outer surfaces.

REFERENCES

[1] N. D. Alikakos, P. W. Bates and X. Chen, Convergence of the Cahn–Hilliard equation to the Hele-Shaw model, *Arch. Rational Mech. Anal.*, **128** (1994), 165–205.

[2] T. Alarcón, H. M. Byrne and P. K. Maini, A cellular automaton model for tumour growth in inhomogeneous environment, *J. Theor. Biol.*, **225** (2003), 257–274.

[3] B. Alberts, A. Johnson, J. Lewis, M. Raff, K. Roberts and P. Walter, *Molecular Biology of the Cell*, 5^{th} edition, Garland Science, New York, 2007.

[4] S. M. Allen and J. W. Cahn, A microscopic theory for antiphase boundary motion and its application to antiphase domain coarsening, *Acta Mater.*, **27** (1979), 1085–1095.

[5] A. R. A. Anderson and M. A. J. Chaplain, Continuous and discrete mathematical models of tumor-induced angiogenesis, *Bull. Math. Biol.*, **60** (1998), 857–899.

[6] A. R. A. Anderson and V. Quaranta, Integrative mathematical oncology, *Nat. Rev. Cancer*, **8** (2008), 227–234.

[7] C. Athale, Y. Mansury and T. S. Deisboeck, Simulating the impact of a molecular 'decision-process' on cellular phenotype and multicellular patterns in brain tumors, *J. Theor. Biol.*, **233** (2005), 469–481.

[8] M. Athanassenas, Volume-preserving mean curvature flow of rotationally symmetric surfaces, *Comment. Math. Helv.*, **72** (1997), 52–66.

[9] K. Bartha and H. Rieger, Vascular network remodeling via vessel cooption, regression and growth in tumors, *J. Theor. Biol.*, **241** (2006), 903–918.

[10] N. Bellomo, N. K. Li and P. K. Maini, On the foundations of cancer modeling: Selected topics, speculations, and perspective, *Math. Models Methods Appl. Sci.*, **18** (2008), 593–646.

[11] M. Brassel and E. Bretin, A modified phase field approximation for mean curvature flow with conservation of the volume, *Math. Meth. Appl. Sci.*, **34** (2011), 1157–1180.
[12] W. L. Briggs, *A Multigrid Tutorial*, SIAM, Philadelphia, 1987.
[13] L. Bronsard and B. Stoth, Volume-preserving mean curvature flow as a limit of a nonlocal Ginzburg–Landau equation, *SIAM J. Math. Anal.*, **28** (1997), 769–807.
[14] H. M. Byrne, A weakly nonlinear analysis of a model of avascular solid tumour growth, *J. Math. Biol.*, **39** (1999), 59–89.
[15] H. M. Byrne, T. Alarcon, M. R. Owen, S. D. Webb and P. K. Maini, Modelling aspects of cancer dynamics: A review, *Phil. Trans. R. Soc. A*, **364** (2006), 1563–1578.
[16] H. M. Byrne and M. A. J. Chaplain, Growth of nonnecrotic tumors in the presence and absence of inhibitors, *Math. Biosci.*, **130** (1995), 151–181.
[17] H. M. Byrne and M. A. J. Chaplain, Growth of necrotic tumors in the presence and absence of inhibitors, *Math. Biosci.*, **135** (1996), 187–216.
[18] H. M. Byrne and M. A. J. Chaplain, Modelling the role of cell-cell adhesion in the growth and development of carcinomas, *Math. Comput. Model.*, **24** (1996), 1–17.
[19] H. M. Byrne and P. Matthews, Asymmetric growth of models of avascular solid tumours: exploiting symmetries, *Math. Med. Biol.*, **19** (2002), 1–29.
[20] J. W. Cahn, C. M. Elliott and A. Novick-Cohen, The Cahn–Hilliard equation with a concentration dependent mobility: motion by minus the Laplacian of the mean curvature, *Eur. J. Appl. Math.*, **7** (1996), 287–301.
[21] J. W. Cahn and J. E. Hilliard, Free energy of a nonuniform system. I. Interfacial free energy, *J. Chem. Phys.*, **28** (1958), 258–267.
[22] E. A. Carlen, M. C. Carvalho and E. Orlandi, Approximate solutions of the Cahn–Hilliard equation via corrections to the Mullins–Sekerka motion, *Arch. Rational Mech. Anal.*, **178** (2005), 1–55.
[23] X. Chen, The Hele-Shaw problem and area-preserving curve-shortening motions, *Arch. Rational Mech. Anal.*, **123** (1993), 117–151.
[24] Y. Chen, S. M. Wise, V. B. Shenoy and J. S. Lowengrub, A stable scheme for a nonlinear, multiphase tumor growth model with an elastic membrane, *Int. J. Numer. Meth. Biomed. Engng.*, **30** (2014), 726–754.
[25] V. Cristini, H. B. Frieboes, X. Li, J. S. Lowengrub, P. Macklin, S. Sanga, S. M. Wise and X. Zheng, Nonlinear modeling and simulation of tumor growth, in *Selected Topics in Cancer Modeling: Genesis, Evolution, Immune Competition, and Therapy* (eds. N. Bellomo, M. Chaplain and E. de Angelis), Birkhäuser, (2008), 113–181.
[26] V. Cristini and J. Lowengrub, *Multiscale Modeling of Cancer: An Integrated Experimental and Mathematical Modeling Approach*, Cambridge University Press, Cambridge, 2010.
[27] V. Cristini, J. Lowengrub and Q. Nie, Nonlinear simulation of tumor growth, *J. Math. Biol.*, **46** (2003), 191–224.
[28] S. Dai and Q. Du, Motion of interfaces governed by the Cahn–Hilliard equation with highly disparate diffusion mobility, *SIAM J. Appl. Math.*, **72** (2012), 1818–1841.
[29] T. S. Deisboeck, L. Zhang, J. Yoon and J. Costa, In silico cancer modeling: Is it ready for prime time?, *Nat. Clin. Pract. Oncol.*, **6** (2009), 34–42.
[30] S. Dormann and A. Deutsch, Modeling of self-organized avascular tumor growth with a hybrid cellular automaton, *In Silico Biol.*, **2** (2002), 393–406.
[31] D. Drasdo, S. Hohme and M. Block, On the role of physics in the growth and pattern formation of multi-cellular systems: what can we learn from individual-cell based models?, *J. Stat. Phys.*, **128** (2007), 287–345.
[32] J. Escher, U. F. Mayer and G. Simonett, The surface diffusion flow for immersed hypersurfaces, *SIAM J. Math. Anal.*, **29** (1998), 1419–1433.
[33] J. Escher and G. Simonett, Classical solutions for Hele-Shaw models with surface tension, *Adv. Differ. Equ.*, **2** (1997), 619–642.
[34] A. Fasano, A. Bertuzzi and A. Gandolfi, Mathematical modelling of tumour growth and treatment, in *Complex Systems in Biomedicine* (eds. A. Quarteroni, L. Formaggia and A. Veneziani), Springer, (2006), 71–108.
[35] H. B. Frieboes, F. Jin, Y.-L. Chuang, S. M. Wise, J. S. Lowengrub and V. Cristini, Three-dimensional multispecies nonlinear tumor growth–II: tumor invasion and angiogenesis, *J. Theor. Biol.*, **264** (2010), 1254–1278.
[36] A. Friedman, Mathematical analysis and challenges arising from models of tumor growth, *Math. Models Methods Appl. Sci.*, **17** (2007), 1751–1772.

[37] P. Gerlee and A. R. A. Anderson, Stability analysis of a hybrid cellular automaton model of cell colony growth, *Phys. Rev. E*, **75** (2007), 051911.
[38] L. Graziano and L. Preziosi, Mechanics in tumor growth, in *Modeling of Biological Materials* (eds. F. Mollica, L. Preziosi and K.R. Rajagopal), Birkhäuser, (2007), 263–321.
[39] H. P. Greenspan, On the growth and stability of cell cultures and solid tumors, *J. Theor. Biol.*, **56** (1976), 229–242.
[40] H. L. P. Harpold, E. C. Alvord and K. R. Swanson, The evolution of mathematical modeling of glioma proliferation and invasion, *J. Neuropath. Exp. Neur.*, **66** (2007), 1–9.
[41] H. Hatzikirou, A. Deutsch, C. Schaller, M. Simon and K. Swanson, Mathematical modelling of glioblastoma tumour development: A review, *Math. Models Methods Appl. Sci.*, **15** (2005), 1779–1794.
[42] G. Huisken, The volume preserving mean curvature flow, *J. Reine Angew. Math.*, **382** (1987), 35–48.
[43] Y. Jiang, J. Pjesivac-Grbovic, C. Cantrell and J. P. Freyer, A multiscale model for avascular tumor growth, *Biophys. J.*, **89** (2005), 3884–3894.
[44] A. R. Kansal, S. Torquato, G. R. Harsh IV, E. A. Chiocca and T. S. Deisboeck, Simulated brain tumor growth dynamics using a three-dimensional cellular automaton, *J. Theor. Biol.*, **203** (2000), 367–382.
[45] J. Kim, S. Lee and Y. Choi, A conservative Allen–Cahn equation with a space–time dependent Lagrange multiplier, *Int. J. Eng. Sci.*, **84** (2014), 11–17.
[46] D.-S. Lee, H. Rieger and K. Bartha, Flow correlated percolation during vascular remodeling in growing tumors, *Phys. Rev. Lett.*, **96** (2006), 058104.
[47] I. M. M. van Leeuwen, C. M. Edwards, M. Ilyas and H. M. Byrne, Towards a multiscale model of colorectal cancer, *World J. Gastroentero.*, **13** (2007), 1399–1407.
[48] X. Li, V. Cristini, Q. Nie and J. S. Lowengrub, Nonlinear three-dimensional simulation of solid tumor growth, *Discrete Cont. Dyn-B*, **7** (2007), 581–604.
[49] J. S. Lowengrub, H. B. Frieboes, F. Jin, Y.-L. Chuang, X. Li, P. Macklin, S. M. Wise and V. Cristini, Nonlinear modelling of cancer: Bridging the gap between cells and tumours, *Nonlinearity*, **23** (2010), R1–R91.
[50] Y. Mansury, M. Kimura, J. Lobo and T. S. Deisboeck, Emerging patterns in tumor systems: Simulating the dynamics of multicellular clusters with an agent-based spatial agglomeration model, *J. Theor. Biol.*, **219** (2002), 343–370.
[51] U. F. Mayer and G. Simonett, Self-intersections for the surface diffusion and the volume-preserving mean curvature flow, *Differ. Integral Equ.*, **13** (2000), 1189–1199.
[52] J. D. Nagy, The ecology and evolutionary biology of cancer: A review of mathematical models of necrosis and tumor cell diversity, *Math. Biosci. Eng.*, **2** (2005), 381–418.
[53] R. L. Pego, Front migration in the nonlinear Cahn–Hilliard equation, *Proc. R. Soc. Lond. A*, **422** (1989), 261–278.
[54] V. Quaranta, A. M. Weaver, P. T. Cummings and A. R. A. Anderson, Mathematical modeling of cancer: The future of prognosis and treatment, *Clin. Chim. Acta*, **357** (2005), 173–179.
[55] B. Ribba, T. Alarcón, P. K. Maini and Z. Agur, The use of hybrid cellular automaton models for improving cancer therapy, in *Cellular Automata* (eds. P.M.A. Sloot, B. Chopard and A.G. Hoekstra), Springer, **3305** (2004), 444–453.
[56] T. Roose, S. J. Chapman and P. K. Maini, Mathematical models of avascular tumor growth, *SIAM Rev.*, **49** (2007), 179–208.
[57] J. Rubinstein and P. Sternberg, Nonlocal reaction–diffusion equations and nucleation, *IMA J. Appl. Math.*, **48** (1992), 249–264.
[58] S. J. Ruuth and B. T. R. Wetton, A simple scheme for volume-preserving motion by mean curvature, *J. Sci. Comput.*, **19** (2003), 373–384.
[59] S. Sanga, H. B. Frieboes, X. Zheng, R. Gatenby, E. L. Bearer and V. Cristini, Predictive oncology: A review of multidisciplinary, multiscale in silico modeling linking phenotype, morphology and growth, *Neurolmage*, **37** (2007), S120–S134.
[60] A. Stuart and A. R. Humphries, *Dynamical System and Numerical Analysis*, Cambridge University Press, Cambridge, 1996.
[61] U. Trottenberg, C. Oosterlee and A. Schüller, *Multigrid*, Academic Press, London, 2001.
[62] S. Turner and J. A. Sherratt, Intercellular adhesion and cancer invasion: A discrete simulation using the extended Potts model, *J. Theor. Biol.*, **216** (2002), 85–100.
[63] S. M. Wise, J. S. Lowengrub and V. Cristini, An adaptive multigrid algorithm for simulating solid tumor growth using mixture models, *Math. Comput. Model.*, **53** (2011), 1–20.

[64] S. M. Wise, J. S. Lowengrub, H. B. Frieboes and V. Cristini, Three-dimensional multispecies nonlinear tumor growth–I: Model and numerical method, *J. Theor. Biol.*, **253** (2008), 524–543.

[65] X. Zheng, S. M. Wise and V. Cristini, Nonlinear simulation of tumor necrosis, neovascularization and tissue invasion via an adaptive finite-element/level-set method, *Bull. Math. Biol.*, **67** (2005), 211–259.

Received October 15, 2014; Accepted July 04, 2015.

E-mail address: leeh@korea.ac.kr
E-mail address: ahyouhappy@gmail.com
E-mail address: cfdkim@korea.ac.kr